Version of Record: https://www.sciencedirect.com/science/article/pii/S0141391020303979
Manuscript_c884206042b4688ee60eb91effbbd4b9

Physical Structure Contributions in pH Degradation of PEO-*b*-PCL Films

Joanna M. White,[a] Justin Jurczyk,[b] and Ryan M. Van Horn[a,b]

[a]Department of Chemical and Biomolecular Engineering, Lafayette College, Easton, PA 18042
[b]Department of Chemistry, Allegheny College, Meadville, PA 16335

Abstract

Poly(ethylene oxide)-*block*-poly(ε-caprolactone) (PEO-*b*-PCL) is an intriguing candidate for hydrophobic drug encapsulation and controlled release into the body as a biocompatible, amphiphilic block copolymer. In this study, a variety of characterization techniques, including DSC, NMR, and SEM, were employed to investigate the degradation of PEO-*b*-PCL films within aqueous environments. Previous work has shown that the degradation of these films is accelerated in both basic and acidic environments; however, it is important to develop a better understanding of degradation rate as it relates to the physical structure of the films. To this end, the degree of crystallinity of each block within PEO-*b*-PCL films was manipulated intentionally by varying the molecular weight and rate of cooling from melt. The data indicated that molecular weight, cooling rate, and pH all have substantial effects on the rate of degradation of the films and the composition of the degradation products over time. In general, increasing the mass fraction or degree of crystallinity of PCL leads to slower degradation. Further, crystallization of the PEO block hinders buffer penetration, slowing degradation, while a higher mass fraction of amorphous PEO accelerates the erosion of these films. This insight can help inform efforts to fine-tune the encapsulation and delivery of hydrophobic pharmaceutical compounds.

© 2020 published by Elsevier. This manuscript is made available under the Elsevier user license
https://www.elsevier.com/open-access/userlicense/1.0/

Introduction

In the 1970s, there was an increased interest in the potential of resorbable, biodegradable polymers for drug-delivery applications [1]. Poly(ε-caprolactone) (PCL), a hydrophobic and semi-crystalline polymer, received significant attention due to ease of processability resulting from good solubility within common non-polar solvents, high blending capability, and low melting point (59-64°C). The polymer was particularly useful for biomedical applications due to the high tunability of its degradation rate, surface structure, and mechanical properties through the incorporation of copolymers or functional groups. Further, the polymer is known to undergo degradation, breaking into monomeric components, via hydrolysis of the ester bonds. As the molecular weight of the polymer increases, however, this degradation process becomes quite slow, taking years to fully degrade under physiological conditions [1–6]. These slow degradation rates limit the applicability of the material for drug-delivery and also present issues associated with the difficulty of determining long-term toxicity of the degradation products [1,2].

After this initial attention, focus moved away from PCL, as other polymers, such as polyglycolide (PGA) and poly(D,L-lactide) (PDLA), have much faster degradation rates (days or weeks as opposed to years) and therefore were more applicable for short-term delivery. It was only in the late 1990s and early 2000s that researchers returned to PCL for biomedical applications because it has improved rheological and viscoelastic properties over these other polymers, making it much easier to process [1-2,4-5].

In recent years, there have been a number of studies that focus on PCL that is copolymerized with poly(ethylene oxide) (PEO) for biomedical applications [4-5,7–23]. This hydrophilic, semi-crystalline polymer been the source of emerging interest within the field of biomaterials because it is nontoxic and can be completely cleared from the body through the kidneys [12]. Interestingly, PEO/PCL copolymers have been shown to exhibit higher degrees of hydrophilicity and faster

degradation rates in comparison to pure PCL [4-5,10–15]. In addition, studies have shown that this degradation is further accelerated by increasing the relative length of the PEO block [5,10–14].

The bulk degradation rate of PCL and its block copolymer with PEO, PEO-*b*-PCL, is highly dependent upon pH. An understanding of these effects is important from a drug-delivery standpoint, as there is a wide-variety of pHs present within the body with highly acidic gastric juices with a pH ranging from 0.9-1.5 and more basic pancreatic juices ranging from pH 7.5-8.2 [3,24]. Studies have shown that the degradation rate of pure PCL films is accelerated in both acidic and basic environments. In acidic environments, the carbonyl group within the PCL is protonated, resulting in nucleophilic attacks from water [3,25,26]. This leads to cleavages within the repeat unit chain, yielding monomer/oligomer products with carboxylic acid and alcohol end groups that are water-soluble. In extremely basic solutions, the hydroxide ions directly attack the carbonyl group, similarly resulting in scission of the repeated chain [25].

Sailema-Palate *et al.* [3] have shown that the degradation rate of pure PCL films in extremely basic environments (pH 13) is significantly faster than that in comparably acidic environments (pH 1). Further, PCL films placed in pH 1 buffer solutions experience an induction period where little mass loss is observed initially. In contrast, films placed in pH 13 buffer solutions immediately begin showing significant mass loss. In addition, the degree of crystallinity increases and average molecular weight decreases over time in the pH 1 buffer, but both remain unchanged in the pH 13 buffer [3].

Loh [4] and Li *et al.* [5] studied the degradation rate of PEO-*b*-PCL films within neutral and basic aqueous buffers. These works observed a similar pattern, with the basic environments accelerating the degradation of the films. In addition to gaining a better understanding of degradation within physiologically-relevant conditions, these extreme pH environments can be

used to accelerate degradation so as to better understand potential toxicology issues associated with the breakdown of these materials [1,4]. At present, little work has been done to investigate the degradation rate of these copolymer films in acidic environments.

In addition to pH, the degree of crystallinity of each semi-crystalline block has an effect on the degradation rate. Due to tight packing, crystalline regions are denser and thus harder for water to penetrate than amorphous regions. *In vivo* and *in vitro* studies have found that amorphous PCL regions undergo hydrolytic degradation at a faster rate than crystalline ones, resulting in a general increase in the degree of crystallinity of the bulk sample over the course of the degradation period [4,5,11,12,15]. Further work by Lam *et al.* [27] has suggested that the surface of PCL films experiences a cyclical increase and decrease in the degree of crystallinity: The amorphous materials degrade, resulting in an increase in the degree of crystallinity, and then the crystalline regions erode away, leaving behind a more amorphous surface. Alexis and coworkers [28,29] have shown that decreased biodegradation rates as a result of a higher degree of crystallinity leads to slower release rates of drugs from polymeric materials into the body.

For PEO-*b*-PCL copolymers, both blocks can crystallize; therefore, the degradation rates or drug release rates of these materials is more complicated. As stated, PCL crystallization inhibits degradation and release. Crystallinity in PEO has been shown to hinder water uptake [14,30–32]. Promotion of water uptake by the PEO block and subsequent infiltration into bulk PCL domains is the main advantage to the application of PEO-*b*-PCL copolymers over homopolymer PCL. As such, understanding the crystallization behavior of both blocks in these copolymers is critical to tailoring desired degradation or release rates.

Numerous studies have been done on the crystallization behavior of PEO-*b*-PCL copolymers [22,33–42]. He *et al.* [22] found that the crystallization order and extent per block within PEO-*b*-

PCL films is directly dependent upon block length. At low weight fractions of PCL ($w_{PCL} < 0.38$), the PEO crystallizes first when cooled from a melt. Following this crystallization, the PCL is able to crystallize to a lesser extent at a lower temperature. As the fraction of PCL increases, the PCL begins to crystallize first, followed by a more limited PEO crystallization. At high PCL fractions ($w_{PCL} > 0.80$), the PEO no longer crystallizes at room temperature. Jiang *et al.* [12] investigated the morphology of PEO-*b*-PCL single crystals ($w_{PCL} = 0.83$). Consistent with the findings from He *et al*. [22], they found that the PEO chains did not crystallize and were present within the amorphous regions at the surface of lamellar PCL crystals. While numerous studies have looked at changes in crystallinity over the course of degradation [4,5,11,12,15], there have been few studies that investigate the effect of the initial crystallinity within each block on the degradation rate of PEO-*b*-PCL films. Jiang *et al.* [12] compared the physical degradation of the PEO-*b*-PCL ($w_{PCL} = 0.83$) to that of homopolymer PCL. While both pure PCL and PEO-*b*-PCL experienced biodegradation from the edges of the crystals, the copolymer additionally experienced significant degradation from the top surface because the tethered amorphous hydrophilic PEO block aided in the transport of water to the crystal's interior. While no significant work has been conducted to date on the effect of double-block crystallinity on the degradation of PEO-*b*-PCL, Albuerne *et al.* [43] investigated the degradation of double-crystalline films prepared from poly(*p*-dioxanone)-*block*-polycaprolactone (PDXX-*b*-PCL). They found that the copolymer formed spherulite crystals with a mixture of each block when cooled from the melt. This structure significantly slowed the degradation rate of the PDXX block within the copolymer in comparison to a film composed of pure PDXX. They believe that the PCL crystals hinder the diffusion of water, slowing the hydrolytic degradation of the PDXX block.

To better assess the feasibility of PEO-*b*-PCL as a biomaterial, this article outlines a systematic study conducted on the degradation of PEO-*b*-PCL films, focusing specifically on the way in which crystallinity, as tailored by molecular weight and cooling rate from the melt, affects the degradation rate and pathway within both acidic and basic environments. PEO-*b*-PCL films were prepared from melt and then degraded under physiologically relevant and extreme pH conditions. The physical and chemical structure of the films over the course of degradation was monitored using DSC, ^{1}H NMR, and SEM.

Experimental Methods

Materials. PEO-*b*-PCL samples of 5,000-5,000 g/mol (5K:5K, PDI = 1.10), 5,000-10,000 g/mol (5K:10K, PDI = 1.2), 5,000-16,300 g/mol (5K:16.3K, PDI = 1.4) and 5,000-24,500 g/mol (5K:24.5K, PDI = 1.3) were purchased from Polymer Source Inc. and used as received. Molecular weight ratios were confirmed using ^{1}H NMR. Buffer solutions of pH 1, 3, 5, 7, 9, and 13 were purchased from LabChem and used as received. Chloroform (99%+ extra pure) was purchased from Acros Organics and used as received.

Sample Preparation. 15 wt % solutions of PEO-*b*-PCL were prepared in chloroform. The polymers readily dissolved in the solvent, resulting in a homogeneous solution. Samples were cast in 5 50-μL aliquots, allowing each aliquot to dry before application of the next, resulting in uniform films of roughly 1 cm in diameter and 1 mm in thickness. After drying in a desiccator overnight, the films were heated on a Mettler Toledo HS-80 hot stage to 90°C for 15 min and recrystallized using one of two methods. For the quench method, the film was removed from the stage and allowed to cool in air to room temperature. For the controlled cool method, the film was cooled at

2°C/min using cold nitrogen gas to 50°C, where it was held isothermally for 15 minutes before being cooled at 2°C/minute to room temperature.

Degradation in pH Buffer Solutions. Dried films were placed into 20-mL glass vials containing 1 mL of the desired buffer solution. The vials were suspended in a hot water bath at 37°C for 24 hrs to mimic physiological conditions. After 24 hrs, films were removed from the buffer solution and placed into a desiccator for an additional 24 hrs. Following desiccation, the dry mass of each film was recorded, a razor blade was used to cut a subsample of known mass (approx. 2-4 mg) for further DSC and SEM analysis, and the remainder was massed and placed in a vial with fresh buffer solution of the initial pH for the next 24-hour duration. This process was repeated for 96 hours or until the film was entirely degraded or eroded (with no pieces able to be recovered using tweezers).

Mass Retention Measurements. The mass retention of the films over the course of degradation was determined using Eqn. 1.

$$\text{Mass Retention } (\%) = \frac{m_t}{m_s} * 100\% \quad (1)$$

where m_t is the total mass of the film at a given time, t, and m_s is the original mass of sample before it was submerged in buffer solution

Differential Scanning Calorimetry (DSC). The thermal properties of the films over the course of degradation were measured using a PerkinElmer DSC 8000 with an Intracooler II attachment. The DSC was calibrated using indium standards, and the mass difference between sample and reference Al pans was less than ±0.1 mg. The measurements were obtained by heating the sample from 30°C to 90°C at a rate of 30°C/minute. The degree of crystallinity of each block was determined from the area under the melting peaks in the first heating segment, assuming

theoretical heats of fusion for 100% crystalline PEO and PCL as 196.6 J/g [44] and 151.7 J/g [45], respectively.

Nuclear Magnetic Resonance Spectroscopy (^{1}H NMR.) A JEOL 400 MHz FT-NMR was used to determine the chemical composition of the degradation products. Following each 24-hour degradation period, the liquid within the pH buffer solutions was evaporated off to obtain the solid degradation products. These solids were redissolved into a 5 mg/mL solution in deuterated chloroform. The relative composition of PEO and PCL present within these products (X_t^{PEO}/X_t^{PCL}) was determined via the ratios of the integration area under the peaks divided by the number of hydrogens that they represent at δ = 3.65 ppm (4 H) and 2.29-2.33 ppm (2 H), respectively. The initial weight fraction of PCL present in the films, w_0^{PCL}, was estimated from the molecular weight. This value was then used alongside the total initial mass of the film, M_0^{Total}, to determine the initial mass of PCL in the film using Eqn. 2.

$$M_0^{PCL} = M_0^{Total} * w_0^{PCL} \tag{2}$$

Eqn. 3 and 4 were used to calculate the mass of PCL lost after being exposed to the aqueous solution for time, t, and the mass fraction of PCL remaining in film, w_t^{PCL}.

$$M_t^{PCL} = M_0^{PCL} - \left(M_0^{Total} - M_t^{Total}\right) * X_t^{PCL} \tag{3}$$

$$w_t^{PCL} = \frac{M_t^{PCL}}{M_t^{Total}} \tag{4}$$

Scanning Electron Microscopy (SEM). The surface structure of the films over the course of degradation was characterized using SEM. Small samples were coated using a gold sputter coater at 30 mA for 20 seconds. Images were obtained using a Nanoscience Instruments Phenom Pro-X SEM at 10 or 15 kV.

Results & Discussion

Because degradation of PCL in PEO-*b*-PCL films is influenced by a number of factors, it is important to evaluate each contributor to the film's erosion. These include, but are not limited to, pH, relative mass fractions of PEO and PCL, and crystallinity of PEO and PCL. The driving force for degradation is the rate of PCL ester bond cleavage. The rate of degradation is, therefore, related to the accessibility of the ester bond to reactive species (protons at low pH or hydroxide ions at high pH). Access is increased with higher concentrations of reactive aqueous ions (more extreme pHs), greater fractions of ester bonds (increased PCL block length), greater water uptake (increased PEO content), and lower density (decreased crystalline PCL content). We investigated how these factors impact degradation for a variety of PEO-*b*-PCL systems. For all of our systems, it was assumed that phase-separation between PEO and PCL was driven by crystallization only resulting in a lamellar-like morphology between blocks. Films were thick; therefore, all crystal morphologies were spherulitic in nature. Because crystallization was characterized by a 3D-spherulitic morphology, both blocks were contained in relatively continuous domains throughout the film.

At pH 7, PEO-*b*-PCL films with PCL weight fractions of 0.67 or less (5K:5K and 5K:10K) achieved 100% mass loss within 24 hours in pH 7 buffer. These films completely dissolved or eroded, making the collection of films for mass retention studies impractical particularly at other pHs. Films with PCL fractions higher than 0.67 (5K:16.3K and 5K:24.5K in particular) experienced less than a 5% mass reduction over a 96 hour period in pH 7 buffer. As a result, these materials are promising candidates for slower delivery of compounds into the body. More detailed studies are being performed on the 5K:5K and 5K:10K systems.

Figure 1 shows mass retention profiles for 5K:24.5K and 5K:16.3K films at various pHs from 1 to 13. Consistent with previously published findings, degradation and erosion was accelerated in

more extreme pH environments [3–5]. As the acidic and basic degradation pathways are dependent upon the concentration of free protons and hydroxide ions within the buffer solutions, this trend is logical. Interestingly, degradation was much faster in the pH 13 buffer (square) than in the comparable pH 1 buffer (diamond), suggesting that the basic degradation mechanism is faster than the acidic one [3]. This is also true when comparing pH 5 (triangles) and pH 9 (crosses) though to a lesser extent. Assuming all other factors are the same, ion concentration increases the mass loss rate of the film.

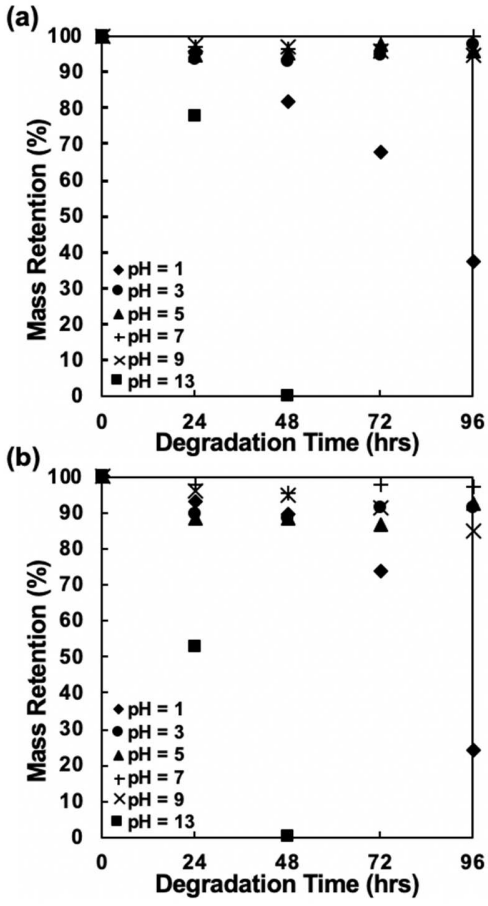


Figure 1. Mass retention as a function of degradation time for (a) 5K:24.5K and (b) 5K:16.3K PEO-*b*-PCL films degraded at various pH. ***(1 column)***

While chemical changes were not studied in great detail, physical differences in the degradation of films at various pH were observed through SEM images of the surface of the

5K:16.3K films after 24 hours shown in Figure 2. As shown, the surface of the film subjected to pH 13 buffer bears prominent pores and fibrous protrusions that resemble lamellar crystals that are not as significant on the surfaces of the films submerged in pH 1 and pH 9 buffers. This is consistent with the mass retention data (Figure 1), as the films submerged in the pH 13 buffer exhibit more rapid erosion and degradation in comparison to those in the pH 1 and 9 buffers.

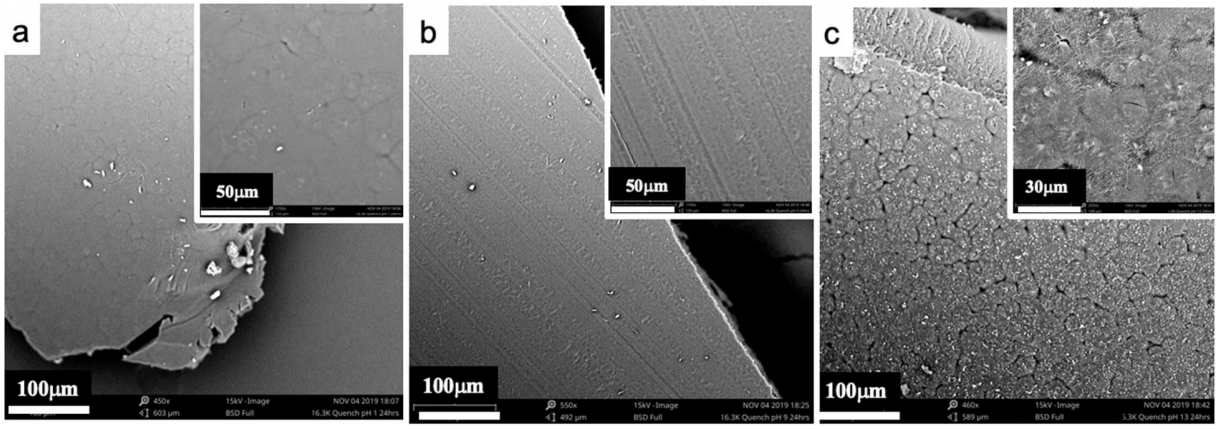


Figure 2. SEM images of 5K:16.3K films degraded in (a) pH 1, (b) pH 9, & (c) pH 13 buffer solutions for 24 hours. ***(2 columns)***

As shown in Figure 1, the 5K:16.3K film loses >75% of its mass when exposed to the pH 1 buffer over 96 hrs. Macroscopic images over the course of degradation show that the film breaks apart into smaller chunks, with entire portions eroding away (Figure S1). Figure 3 shows SEM images of films degraded for 96 hrs in pH 1 and pH 9 buffer solutions. Figure 3a shows that the eroded chunks remain intact with a porous structure. This suggests that much of the mass loss shown in Figure 1 was facilitated by erosion as opposed to pure degradation. Differences in physical degradation at extreme pH is further evident within the pH 1 and pH 9 (Figure 3b) buffer after 96 hours. In contrast to the changes in surface structure present in the film placed in the pH

1 buffer, the film in the pH 9 buffer does not show significant physical changes after 96 hours. This demonstrates that in pH 9, erosion and degradation are minimal.

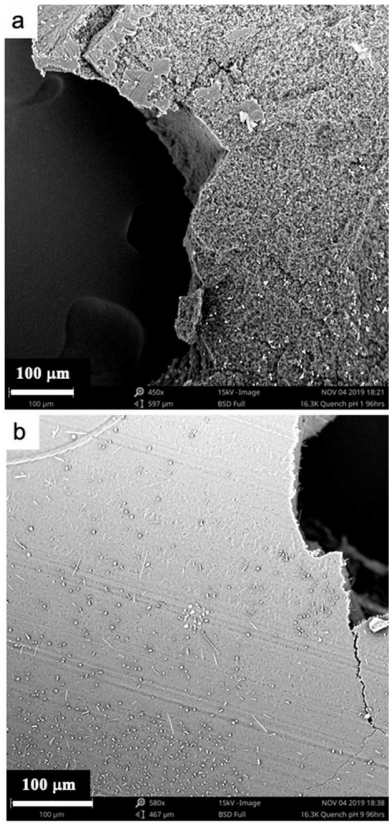


Figure 3. SEM images of 5K:16.3K films degraded in (a) pH 1 & (b) pH 9 buffer solutions for 96 hours. ***(1 column)***

Consistent with previously published work, films with higher fractions of PCL exhibited slower degradation within both acidic and basic environments [5, 10-14]. Figure 4 shows mass retention profiles for 5K:16.3K (diamonds) and 5K:24.5K (squares) films at pH 1, 9, and 13. Films are expected to undergo initial mass loss through solvation and erosion of the hydrophilic PEO block facilitated by PCL chain scission near the junction point of the block copolymer. This erosion leads to cavities in the film that expose the PCL block, making it more susceptible to hydrolytic degradation through ester scission. With a higher fraction of PEO, erosion is more substantial, resulting in accelerated ester cleavage and degradation. This is particularly evident for the films in

the pH 9 buffer (Figure 4b). As shown, degradation was slow within both films. After 24 hours, however, the 5K:16.3K film exhibited significantly faster mass loss in comparison to the 5K:24.5K film, resulting in mass loss after 96 hours of 15% and 5%, respectively. Similar results were found for pH 13 (Figure 4c), where the mass loss of the 5K:24.5K film after 24 hours is 22% and 48% for the 5K:16.3K film. Both of the films were eroded entirely after 48 hours in the pH 13 buffer. As measurements were only taken every 24 hours, it is difficult to know precisely when each of the films was entirely degraded. Interestingly, pH 1 showed that degradation was comparable for the two samples through 72 hrs. While the results are not as clear at pH 1, after 96 hours, the same trend was found, with the final percent mass loss of the 5K:24.5K and 5K:16.3K films at 62% and 76%, respectively.

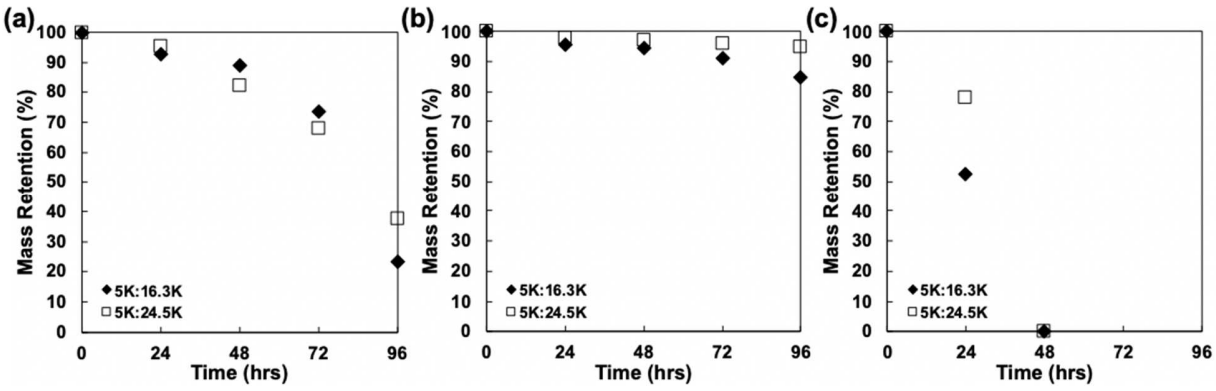


Figure 4. Mass retention as a function of degradation time for 5K:16.3K (diamonds) and 5K:24.5K (squares) films in (a) pH 1 buffer, (b) pH 9 buffer, and (c) pH 13 buffer. ***(2 columns)***

The mass loss analyses shown in Figures 1 – 4 demonstrate that both ion concentration and PEO/PCL content are important factors in the degradation rate of PEO-*b*-PCL copolymer films. What is less clear is how crystallinity of both PEO and PCL blocks impacts the observed rates. To systematically probe the effect of crystallinity, tailored by molecular weight and cooling rate on the degradation of these films, the remainder of this study focused on films in pH 1, 9, and 13 buffers. While milder pH environments can provide insight into longer-term degradation in more

neutral, physiologically-relevant conditions, the degradation mechanism may differ slightly than this model at more extreme pHs given that the process is controlled by both thermodynamic and kinetic considerations related to solvent absorption, chain mobility, and reactivity.

In addition to PEO domain size and ester bond availability, the molecular weight of each block has an impact on the initial crystallization of the films (Table 1). Crystallinity was determined using DSC using Equation 5:

$$\chi_c = \frac{\Delta H_m}{w \Delta H_m^o} \quad (5)$$

where χ_c is the crystallinity for the given block, ΔH_m is the heat of melting measured by DSC, w is the weight fraction of the given block, and ΔH_m^o is the heat of melting for the 100% crystalline block. Representative thermograms of as-cast films can be found in the Supporting Information (Figure S2). The heating curves of the 5K:24.5K films shows a single, wide peak ranging from ~55–65°C. The large width of this peak can be attributed to variation in the thickness of the crystals within the film resulting from the quick quench cooling method used during casting. The area under this entire peak was used to determine the percent of crystallinity within the PCL block as PEO is known to not crystallize above room temperature in this copolymer (39). The 5K:16.3K film exhibited a narrower peak at 60°C (PCL melting) with a shoulder at 50°C attributed to PEO melting. To reduce error associated with calculating the ΔH_m with peak overlap, the area from the top of the peak to the return to the baseline on the right side was doubled and used to estimate the degree of crystallinity of the PCL block. Similarly, the area from the top of the shoulder to the baseline on the left side was doubled and used to estimate the degree of crystallinity of the PEO block. Consistent with He *et al.* [22], PCL exhibited a lower crystallinity (χ_c) at lower mass fractions. χ_c^{PCL} for the 5K:16.3K sample quenched to room temperature was 40.6%, whereas χ_c^{PCL} for 5K:24.5K was 45.0%. Additionally, the 5K:16.3K PEO chains exhibited crystallization to a

small extent. In contrast, with a higher fraction of PCL (5K:24.5K sample), the PEO was unable to crystallize at all under the cooling procedure utilized here. Dry samples of 5K:5K and 5K:10K typically have larger χ_c^{PEO} due to coincident crystallization, though the exact amount is difficult to evaluate [46]. As water has been shown to dissolve PEO crystals, both in homopolymers and copolymers, it is likely that this higher degree of crystallinity has minimal effect on hydration and erosion of samples compared to copolymers with higher PCL weight fraction [32]. When PCL weight fraction is small enough, the PEO moiety facilitates dissolution of copolymer chains to accelerate film breakdown; however, when PCL is the significant majority component, as it is for 5K16.3K and 5K24.5K, high levels of film erosion are controlled by the PCL chain degradation. The interplay of PEO dissolution and PCL crystal disassembly makes the faster erosion of the 5K:5K and 5K:10K samples interesting and the subject of further study elsewhere.

Table 1. Initial degree of crystallinity for 5K:16.3K and 5K:24.5K films.

Sample	χ_c PCL	χ_c PEO
5K:16.3K	40.6%	30.7%
5K:24.5K	45.0%	0%

As discussed previously, the 5K:24.5K films exhibit slower mass loss in comparison to the 5K:16.3K films. Some of this difference can be attributed to a lower fraction of the hydrophilic PEO, resulting in a decreased ability of water to permeate the film through this block. Differences in the degree of crystallinity of each of these films additionally impacts these degradation profiles. As crystallinity is known to hinder diffusion of water and access to ester bonds for degradation, the higher χ_c^{PCL} within the 5K:24.5K films makes the PCL block chains less prone to degradation than the PCL block within the 5K:16.3K film [4,5,11,12,15]. Additionally, higher χ_c^{PEO} also slows water permeation and degradation. However, the faster degrading 5K:16.3K films exhibit significant degrees of crystallinity while the PEO block within the 5K:24.5K films do not. In this

case, the crystallinity effect is not strong enough to overwhelm more prominent composition and χ_c^{PCL} effects, resulting in the 5K:16.3K films still exhibiting a faster degradation profile than the 5K:24.5K films. Further probing of these crystallinity effects will be discussed later in this article.

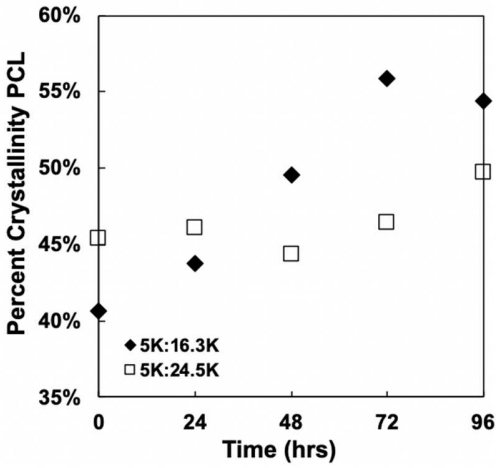


Figure 5. χ_c^{PCL} as a function of degradation time for 5K:16.3K and 5K:24.5K films degraded in pH 9 buffer. ***(1 column)***

Consistent with previously published results, the films of both molecular weights experienced an increase in degree of PCL crystallinity over the course of degradation [4,5,11,12,13]. Figure 5 shows the change in χ_c^{PCL} with time in pH 9 buffer for 5K:16.3K (diamonds) and 5K:24.5K (squares) as measured by DSC. Representative DSC thermograms after degradation can be found in the Supporting Information (Figure S3). This fairly neutral buffer was useful to examine because degradation was slow enough to show substantial differences in crystallinity between the two samples. In general, χ_c^{PCL} increased rapidly for 5K:16.3K and more slowly for 5K:24.3K. The tight packing structure of crystalline PCL inhibits penetration of the reactive species. As a result, much of the initial degradation occurred within the more accessible amorphous regions. As the amorphous regions degrade and erode away, the overall degree of crystallinity of the remaining film increased. This erosion is shown in Figure 6. The surface of the as-cast film is featureless.

After 72 hours, cavities and defined structures resembling crystalline lamellae are present. As shown in Table 1, the PEO block initially crystallizes within the 5K:16.3K film; however, the peak associated with PEO crystallization on the DSC traces disappeared following 24 hours of degradation in any of the buffer solutions. As will be discussed in more detail in a later section, the hydrophilic PEO block erodes more quickly than the PCL block, resulting in a decrease in the fraction of PEO in the film over time. Since the fraction of PEO is already much smaller than that of PCL in the initial film, erosion of the PEO block during the initial 24 hours results in a film with nearly no PEO crystallization.

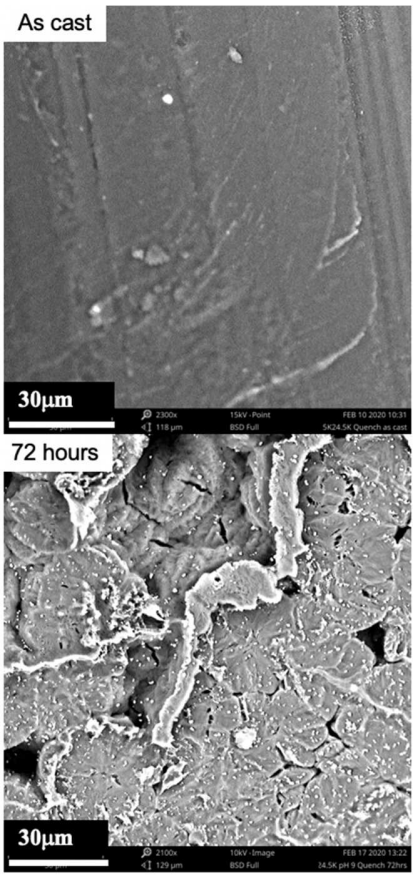


Figure 6. SEM images of 5K:24.5K film prepared *via* the quench method as-cast and after 72 hours in the pH 9 buffer. ***(1 column)***

The 5K:24.5K film exhibited a lag period and a slight decrease in crystallinity before an ultimate increase. This phenomenon can be understood through examination of the ^{1}H NMR

spectra of the degradation products, which are shown in Figure 7. Due to the slower degradation of the 5K:24.5K film relative to the 5K:16.3K film, PCL did not begin to appear in the degradation products of the former until 72 hours. Before this time, only PEO was eroding away, which did not have an impact on the crystallinity of the PCL regions. This seems to indicate that solvation of PEO and cleavage near the PEO-PCL junction point occurred during the initial exposure to aqueous solution. In contrast, in the 5K:16.3K film, significant PCL has degraded away by 48 hours. As discussed, this initial PCL degradation occurred primarily in the amorphous regions. Because PCL was less crystalline in the 5K:16.3K film, the quicker increase in degree of crystallinity was driven by degradation of these amorphous regions.

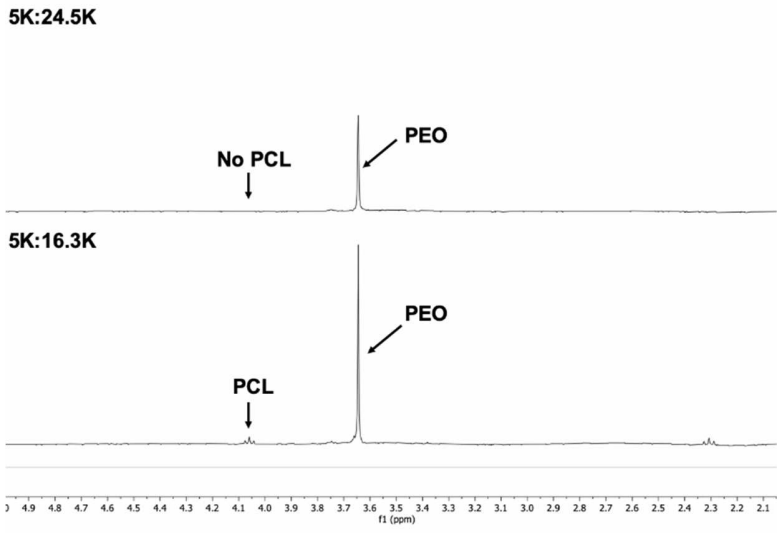


Figure 7. ^{1}H NMR spectra of degradation products from 5K:24.5K (top) and 5K:16.3K (bottom) films after 48 hours in pH 9 buffer. ***(1.5 columns)***

Influence of Single-Block Crystallization – 5K:25.4K. DSC traces of the first heating curve for 5K:24.5K films (Figure S4) show that the average degree of crystallinity within the PCL block is higher for those prepared using the controlled cooling method in comparison to those prepared via the quench method. For the quench film, χ_c^{PCL} was 44% ± 2% and T_m^{PCL} was 60.3°C ± 1.3°C. The shape of the quench curve suggests that melt-recrystallization may have occurred in the least stable (thinnest) crystals within these films. This means that the actual χ_c for the quench films is

likely slightly smaller than the calculated value. During preparation, the controlled-cool films were cooled from 90°C at 2°C/min and held at 50°C for 15 minutes. Here, the chains were able to form thicker nuclei before being slowly cooled to room temperature. Because there were thicker, more stable nuclei, a higher degree of crystallinity and higher T_m were achieved. This method proved to be reproducible, providing films with an average χ_c^{PCL} of 51% ± 2% and a T_m^{PCL} of 63.1°C ± 0.4°C. In addition, based on DSC curves, the distribution of crystal sizes is more narrow with fewer thin, less stable PCL crystals.

The goal of manipulating the degree of crystallinity was to probe ways to affect intentionally the degradation process within the films. Figure 8(a) shows the mass loss profiles for the quench films (open symbols) compared to the controlled cool films (closed symbols) of 5K:24.5K at varying pH. Consistent with Alexis *et al.* [28, 29], the films prepared *via* the controlled cool method that achieve a higher degree of PCL crystallinity exhibit slower mass loss than those prepared using the quench method.

To better assess the material's potential as a drug-delivery agent, it is important to understand the rate of degradation of each block individually as well as the entire film. Figure 8(b) shows the w_t^{PCL} remaining in the film (as determined via ^{1}H NMR and Eqns. 2-4), as a function of time, pH, and preparation method. Interestingly, despite the higher degree of crystallinity within the controlled-cool films (closed symbols), the mass fraction of PCL remaining in the films as a function of degradation time is higher for the quench films (open symbols) in comparison to the controlled-cool films.

SEM images of these films, as shown in Figure 8(c), suggest that this might be due, in part, to differences in the surface composition and structure of the films following casting. There is the appearance of lamelle-like protrusions reminiscent of spherulitic morphologies present in the as-

cast films prepared using the controlled cool method, while the quenched film's surface appears featureless immediately after being cast. This suggests that the controlled cool method led to higher surface roughness likely due to crystals preferentially locating themselves on the surface, serving as a barrier that prevented the solution from eroding away more PEO, resulting in less of an increase in the PCL fraction within the film. In addition, the more crystalline PCL within the controlled-cool films may enhance PEO anchoring, further reducing solubilization of the PEO/PCL chains.

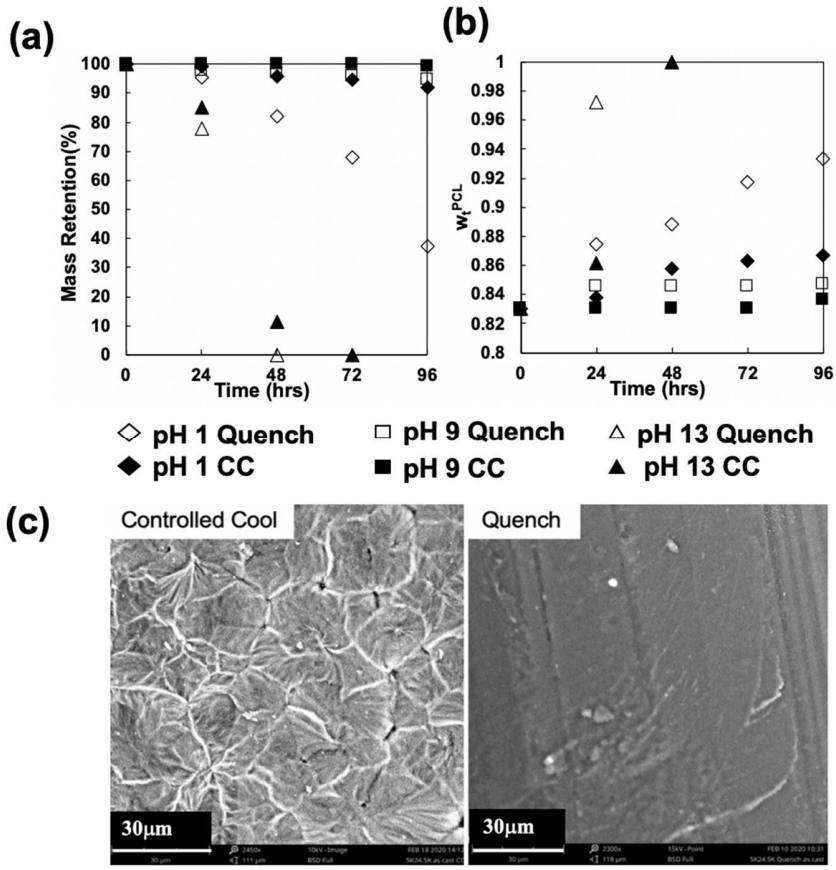


Figure 8. (a) Mass retention over time for 5K:24.5K films prepared *via* the controlled cool (closed symbols) and quench (open symbols) methods degraded in buffer solutions at different pH (b) Mass fraction of PCL remaining in the 5K:24.5K film as a function of degradation time as determined using ^{1}H NMR (c) SEM images of 5K:24.5K films prepared via the controlled cool and quench methods. ***(1.5 columns)***

Influence of Double-Block Crystallization - 5K:16.3K. In contrast to the 5K:24.5K films, both the PEO and PCL blocks crystallize within the 5K:16.3K films. DSC measurements showed that films prepared via the quench method had slightly lower χ_c^{PCL} and T_m^{PCL} in comparison to the controlled cool films, indicating that the crystals are less thick (Table 2). This lower degree of crystallinity and thinner crystals allows for more movement of the PEO chains, leading to higher χ_c^{PEO} for the quench films relative to the controlled cool films.

Table 2. Thermal characterization of 5K:16.3K films as determined via DSC using the first heating scan

Method	χ_c^{PCL}	T_m^{PCL} (°C)	χ_c^{PEO}	T_m^{PEO} (°C)
Controlled Cool	43%	62.0	13%	51.5
Quench	40%	59.7	31%	48.6

Figure 9(a) shows the mass retention of the 5K:16.3K films with different cooling procedures stored in pH 1, 9, & 13 buffers. As shown, the films prepared using the controlled cool method (closed symbols) exhibited a faster degradation than those prepared using the quench method (open symbols). This is a contrasting effect to what was found in the 5K:24.5K films and consistent with findings from Albuerne *et al.* [43]. This difference is attributed to the crystallization of PEO within the 5K:16.3K films. The higher χ_c^{PEO} within the 5K:16.3K quench films inhibited penetration of the buffer solution into the film, resulting in slowed degradation relative to the controlled-cool films [14, 30-32].

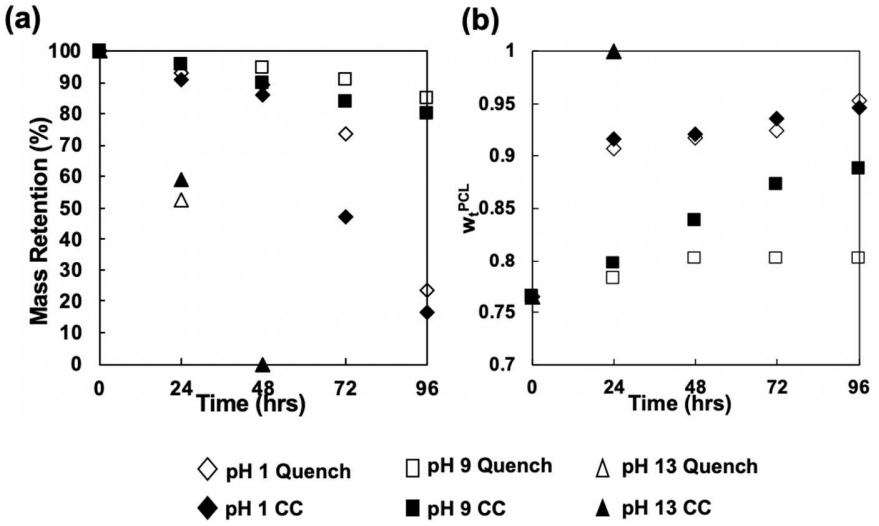


Figure 9. (a) Mass retention as a function of degradation time for 5K:16.3K films prepared via the controlled cool (closed symbols) and quench (open symbols) methods. (b) Mass fraction of PCL remaining in 5K:16.3K films prepared using the quench and controlled cool methods as a function of degradation time in pH 1, 9, and 13 buffers. ***(1.5 columns)***

*Note: the data points at pH 13 are identical for the films prepared using the quench and controlled-cool methods.

Again, the composition of the degradation products helps elucidate the degradation pathway of the film. Figure 9(b) shows the w_t^{PCL} change for 5K:16.3K. As expected, w_t^{PCL} within the films increased over time within all pH, regardless of the crystallization method employed. Particularly evident for the films in the pH 9 buffer (square), w_t^{PCL} increased more rapidly in the controlled-cool films (closed symbols) than the quench films (open symbols). The quench films had a higher χ_c^{PEO} relative to the controlled-cool films. The greater degree of crystallinity within this hydrophilic block slowed PEO erosion. While this leads to slower overall degradation, once PEO erosion does occur, χ_c^{PCL} was lower, increasing the ability of the buffer to cleave the ester bonds within the PCL. In contrast, although the more amorphous PEO allowed for accelerated PEO erosion within the controlled-cool films, the higher χ_c^{PCL} hindered ester cleavage, resulting in a more rapid increase in w_t^{PCL} in the film. This is further confirmed through the ^{1}H NMR spectra of the degradation products (Figure S5). In the pH 9 buffer, PCL did not occur in the controlled-cool

degradation products in a high enough concentration to appear on the spectra. In contrast, PCL was noticeably present in the quench products from 48 hours onwards. This interplay between the roles of PEO and PCL crystallinity greatly influences the degradation behavior. If the crystallization were controlled in a more robust way, the degradation rate could be tuned for a variety of applications.

Conclusion

Molecular weight, pH of the surrounding environment, and crystallinity have a substantial impact on the rate and pathway of degradation for PEO-*b*-PCL films. Hydrolytic degradation within PEO-*b*-PCL films begins with erosion within the hydrophilic PEO block. This erosion creates pores on the surface of the film that expose the PCL blocks. The latter undergo ester cleavage, resulting in a breakdown of the films into soluble oligomers and monomers. Unsurprisingly, the rate of degradation is accelerated with higher weight fractions of PEO. This is attributed to faster buffer penetration, which is associated with higher fractions of the hydrophilic block and with smaller fractions of PCL crystallizing to a lesser degree. In addition, due to their more rapid degradation, the films composed of lower fractions of PCL have PCL appearing in their degradation products at an earlier time.

While degradation of PEO-*b*-PCL films is accelerated in both basic and acidic environments, mass loss is particularly rapid in extremely basic buffers. Degradation is likely to occur first within the amorphous portions of the films. Therefore, it is unsurprising that in all buffers, but particularly at pH 13, there is an increase in the degree of crystallinity and homogeneity of the crystal thickness over time. Interestingly, the 5K:24.5K films in the pH 13 buffer degrade entirely after 48 hours, but no PCL is present in the degradation products until the second 24-hour period. As a hydrophobic drug would be incorporated into the PCL block, this would result in complete delivery

during the second 24-hour period. In contrast, within the pH 1 buffer, the film degrades much less rapidly, but exhibits a more constant degradation rate of PCL from 48 hours onwards. This has the potential to produce a continuous, extended-delivery profile.

The cooling rate used when casting PEO-*b*-PCL films has an effect on the degradation rate and composition of the degradation products. For high weight fractions of PCL, where PCL is the only block to crystallize, slowing the cooling rate from the melt results in an increase in the degree of crystallinity within the PCL block. This higher degree of crystallinity hinders buffer penetration, slowing overall degradation. For lower weight fractions of PCL, both the PEO and the PCL blocks exhibit crystallinity. Again, a slower cooling rate results in an increase in PCL crystallinity, but here, that forces a decrease in PEO crystallinity. It is easier for the buffer solution to penetrate into the more amorphous PEO within the controlled-cool films, resulting in faster overall degradation relative to the quench films. Despite overall faster mass loss, the rate of PCL degradation is significantly slower in the controlled-cool films because the higher degree of PCL crystallinity hinders ester cleavage.

By varying the molecular weight and degree of crystallinity of each block within PEO-*b*-PCL films, a wide array of overall and component degradation profiles can be accessed. As PEO-*b*-PCL is an FDA-approved amphiphilic block-copolymer, these variable degradation profiles can be harnessed to serve as vehicles for controlled and targeted drug delivery of both hydrophilic and hydrophobic compounds.

Acknowledgements

The authors would like to thank the National Science Foundation (DMR-1839762) for support on this project. The authors also would like to thank the Chemistry Department at Lafayette College and Professor Xiaodong Fan for help with the NMR experiments.

References

[1] M.A. Woodruff, D.W. Hutmacher, The return of a forgotten polymer - Polycaprolactone in the 21st century, Prog. Polym. Sci. 35 (2010) 1217–1256.

[2] A.L. Sisson, D. Ekinci, A. Lendlein, The contemporary role of caprolactone chemistry to create advanced polymer architectures, Polymer 54 (2013) 4333–4350.

[3] G.P. Sailema-Palate, A. Vidaurre, A.F. Campillo, I. Castilla-Cortázar, A comparative study on Poly(ϵ-caprolactone) film degradation at extreme pH values, Polym. Degrad. Stab. 130 (2016) 118–125.

[4] X.J. Loh, The effect of pH on the hydrolytic degradation of poly(ε-caprolactone)-block-poly(ethylene glycol) copolymers, J. Appl. Polym. Sci. 127 (2013) 2046–2056.

[5] S.M. Li, X.H. Chen, R.A. Gross, S.P. Mccarthy, Hydrolytic degradation of PCL/PEO copolymers in alkaline media, J. Mater. Sci. Mater. Med. 11 (2000) 227–233.

[6] H. Sun, L. Mei, C. Song, X. Cui, P. Wang, The in vivo degradation, absorption and excretion of PCL-based implant, Biomaterials. 27 (2006) 1735–1740.

[7] Y. Geng, D.E. Discher, Hydrolytic degradation of poly(ethylene oxide)-block-polycaprolactone worm micelles, J. Am. Chem. Soc. 127 (2005) 12780–12781.

[8] H. Danafar, MPEG-PCL copolymeric nanoparticles in drug delivery systems, Cogent Med. 3 (2016).

[9] W. Qi, P.P. Ghoroghchian, G. Li, D.A. Hammer, M.J. Therien, Aqueous self-assembly of poly(ethylene oxide)-block-poly(ε-caprolactone) (PEO-b-PCL) copolymers: Disparate diblock copolymer compositions give rise to nano- and meso-scale bilayered vesicles, Nanoscale 5 (2013) 10908-10915.

[10] K. Gorna, S. Gogolewski, Biodegradable polyurethanes for implants. II. In vitro degradation and calcification of materials from poly(ε-caprolactone)-poly(ethylene oxide) diols and various chain extenders, J. Biomed. Mater. Res. 60 (2002) 592–606.

[11] M.-H. Huang, S. Li, D.W. Hutmacher, J.-T. Schantz, C.A. Vacanti, C. Braud, M. Vert, Degradation and cell culture studies on block copolymers prepared by ring opening polymerization of ε-caprolactone in the presence of poly(ethylene glycol), J. Biomed. Mater. Res. 69A (2004) 417–427.

[12] N. Jiang, S. Jiang, Y. Hou, S. Yan, G. Zhang, Z. Gan, Influence of chemical structure on enzymatic degradation of single crystals of PCL-b-PEO amphiphilic block copolymer, Polymer 51 (2010) 2426–2434.

[13] F. He, S. Li, M. Vert, R. Zhuo, Enzyme-catalyzed polymerization and degradation of copolymers prepared from ε-caprolactone and poly(ethylene glycol), Polymer 44 (2003) 5145–5151.

[14] J.-Z. Bei, J.-M. Li, Z.-F. Wang, J.-C. Le, S.-G. Wang, Polycaprolactone-poly(ethylene-glycol) block copolymer. IV: Biodegradation behavior in vitro and in vivo, Polym. Adv. Technol. 8 (1997) 693–696.

[15] M. Ponjavic, M.S. Nikolic, J. Nikodinovic-Runic, S. Jeremic, S. Stevanovic, J. Djonlagic, Degradation behaviour of PCL/PEO/PCL and PCL/PEO block copolymers under controlled hydrolytic, enzymatic and composting conditions, Polym. Test. 57 (2017) 67–77.

[16] H. Hyun, Y.H. Kim, I.B. Song, J.W. Lee, M.S. Kim, G. Khang, K. Park, H.B. Lee, In vitro and in vivo release of albumin using a biodegradable MPEG-PCL diblock copolymer as an in situ gel-forming carrier, Biomacromolecules. 8 (2007) 1093–1100.

[17] M.S. Kim, K.S. Seo, G. Khang, S.H. Cho, H.B. Lee, Preparation of poly(ethylene glycol)-

block-poly(caprolactone) copolymers and their applications as thermo-sensitive materials, J. Biomed. Mater. Res. 70A (2004) 154–158.
[18] C. Hua, C.-M. Dong, Synthesis, characterization, effect of architecture on crystallization of biodegradable poly(ε-caprolactone)-b-poly(ethylene oxide) copolymers with different arms and nanoparticles thereof, J. Biomed. Mater. Res. Part A. 82A (2007) 689–700.
[19] Z. Ma, A. Haddadi, O. Molavi, A. Lavasanifar, R. Lai, J. Samuel, Micelles of poly(ethylene oxide)-b-poly(ε-caprolactone) as vehicles for the solubilization, stabilization, and controlled delivery of curcumin, J. Biomed. Mater. Res. - Part A. 86 (2008) 300–310.
[20] D.B. Shenoy, M.M. Amiji, Poly(ethylene oxide)-modified poly(ε-caprolactone) nanoparticles for targeted delivery of tamoxifen in breast cancer, Int. J. Pharm. 293 (2005) 261–270.
[21] X.B. Xiong, A. Mahmud, H. Uludağ, A. Lavasanifar, Conjugation of arginine-glycine-aspartic acid peptides to poly(ethylene oxide)-b-poly(ε-caprolactone) micelles for enhanced intracellular drug delivery to metastatic tumor cells, Biomacromolecules. 8 (2007) 874-884.
[22] C. He, J. Sun, C. Deng, T. Zhao, M. Deng, X. Chen, X. Jing, Study of the synthesis, crystallization, and morphology of poly(ethylene glycol) - poly(ε-caprolactone) diblock copolymers, Biomacromolecules 5 (2004) 2042–2047.
[23] Y. Hu, L. Zhang, Y. Cao, H. Ge, X. Jiang, C. Yang, Degradation behavior of poly(ε-caprolactone)-b-poly(ethylene glycol)-b-poly(ε-caprolactone) micelles in aqueous solution, Biomacromolecules 5 (2004) 1756–1762.
[24] C.C.D. Chu, C.C. Chu, E. Analysis, M. Van, R. Hall, A comparison of the effect of pH on the biodegradation of two synthetic absorbable sutures from the department of design, Ann Surg. 195 (1982) 55–59.
[25] L.N. Woodard, M.A. Grunlan, Hydrolytic degradation and erosion of polyester biomaterials, ACS Macro Lett. 7 (2018) 976–982.
[26] J.E. Pickett, D.J. Coyle, Hydrolysis kinetics of condensation polymers under humidity aging conditions, Polym. Degrad. Stab. 98 (2013) 1311–1320.
[27] C.X.F. Lam, M.M. Savalani, S.-H. Teoh, D.W. Hutmacher, Dynamics of in vitro polymer degradation of polycaprolactone-based scaffolds: accelerated versus simulated physiological conditions, Biomed. Mater. 3 (2008) 034108.
[28] F. Alexis, Factors affecting the degradation and drug-release mechanism of poly(lactic acid) and poly[(lactic acid)-co-(glycolic acid)], Polym. Int. 54 (2005) 36–46.
[29] F. Alexis, S. Venkatraman, S.K. Rath, F. Boey, In vitro study of release mechnaisms of paclitxel and rapamycin from drug-incorporated biodegradable stent matrices, J. Control. Release. 98 (2004) 67–74.
[30] B. Gebben, A water vapor-permeable membrane from block copolymers of poly (butylene terephthalate) and polyethylene oxide, J. Memb. Sci. 113 (1996) 323–329.
[31] O. Oparaji, M. Minelli, C. Zhu, E. Schaible, A. Hexemer, D.T. Hallinan, Effect of block copolymer morphology on crystallization and water transport, Polymer 120 (2017) 209–216.
[32] O. Oparaji, X. Zuo, D.T. Hallinan, Crystallite dissolution in PEO-based polymers induced by water sorption, Polymer 100 (2016) 206–218.
[33] L. Li, F. Meng, Z. Zhong, D. Byelov, W.H. De Jeu, J. Feijen, Morphology of a highly asymmetric double crystallizable poly (ε -caprolactone- b -ethylene oxide) block copolymer, J. Chem. Phys. 126 (2007) 024904.

[34] B. Bogdanov, A. Vidts, E. Schacht, H. Berghmans, Isothermal Crystallization of Poly(ε-caprolactone−ethylene glycol) Block Copolymers, Macromolecules 32 (1999) 726–731.
[35] Y. Suzuki, H. Duran, M. Steinhart, H.J. Butt, G. Floudas, Suppression of poly(ethylene oxide) crystallization in diblock copolymers of poly(ethylene oxide)-b-poly(ε-caprolactone) confined to nanoporous alumina, Macromolecules 47 (2014) 1793–1800.
[36] Y. Xu, Y. He, J. Wei, Z. Fan, S. Li, Morphology and melt crystallization of PCL-PEG diblock copolymers, Macromol. Chem. Phys. 209 (2008) 1836–1844.
[37] A.J. Müller, M.L. Arnal, F. López-Carrasquero, Nucleation and crystallization of PS-b-PEO-b-PCL triblock copolymers, Macromol. Symp. 183 (2002) 199–204.
[38] Z.-X. Du, J.-T. Xu, Z.-Q. Fan, Regulation of micellar morphology of PCL-b-PEO block copolymers by crystallization temperature, Macromol. Rapid Commun. 26 (2008) 467-471.
[39] N. Brigham, C. Nardi, A. Carandang, K. Allen, R.M. Van Horn, Manipulation of crystallization sequence in PEO- b -PCL films using solvent interactions, Macromolecules 50 (2017) 8996–9007.
[40] C. He, J. Sun, T. Zhao, Z. Hong, X. Zhuang, X. Chen, X. Jing, Formation of a unique crystal morphology for the poly(ethylene glycol)-poly(ε-caprolactone) diblock copolymer, Biomacromolecules 7 (2006) 252–258.
[41] M.L. Arnal, F. López-Carrasquero, E. Laredo, A.J. Müller, Coincident or sequential crystallization of PCL and PEO blocks within polystyrene-b-poly(ethylene oxide)-b-poly(ε-caprolactone) linear triblock copolymers, Eur. Polym. J. 40 (2004) 1461–1476.
[42] J. Sun, C. He, X. Zhuang, X. Jing, X. Chen, The crystallization behavior of poly(ethylene glycol)-poly(ε- caprolactone) diblock copolymers with asymmetric block compositions, J. Polym. Res. 18 (2011) 2161–2168.
[43] J. Albuerne, L. Marquez, A.J. Müller, J.-M. Raquez, P. Degée, P. Dubois, Hydrolytic Degradation of Double Crystalline PPDX-b-PCL Diblock Copolymers, Macromol. Chem. Phys. 206 (2005) 903–914.
[44] E. Araneda, A. Leiva, L. Gargallo, N. Hadjichristidis, I. Mondragon, D. Radic, Crystallization behavior of PEO in blends of poly(ethylene oxide)/poly(2-vinyl pyridine)-*b*-(ethylene oxide) block copolymer, Polym. Eng. & Sci. 52 (2011) 1128-1136.
[45] A. Wurm, E. Zhuravlev, K. Eckstein, D. Jehnichen, D. Pospiech, R. Androsch, B. Wunderlich, C. Schick, Crystallization and homogenous nucleation kinetics of poly(ε-caprolactone) (PCL) with different molar masses, Macromolecules 45 (2012) 3816–3828.
[46] C. He, J. Sun, J. Ma, X. Chen, X. Jiang, Composition dependence of the crystallization behavior and morphology of the poly(ethylene oxide)-poly(e-caprolactone) diblock copolymer, Biomacromolecules 7 (2006) 3482-3489